

Automatika

Journal for Control, Measurement, Electronics, Computing and Communications



ISSN: 0005-1144 (Print) 1848-3380 (Online) Journal homepage: <https://www.tandfonline.com/loi/taut20>

Induction motor speed control using reduced-order model

A. Sabir & S. Ibrir

To cite this article: A. Sabir & S. Ibrir (2018) Induction motor speed control using reduced-order model, *Automatika*, 59:3-4, 274-285, DOI: [10.1080/00051144.2018.1531963](https://doi.org/10.1080/00051144.2018.1531963)

To link to this article: <https://doi.org/10.1080/00051144.2018.1531963>



© 2018 The Author(s). Published by Informa UK Limited, trading as Taylor & Francis Group



Published online: 23 Oct 2018.



[Submit your article to this journal](#)



Article views: 397



[View related articles](#)



[View Crossmark data](#)



Induction motor speed control using reduced-order model

A. Sabir^a and S. Ibrir^b

^aDepartment of Electrical Engineering, University of Hafr Al Batin, Hafr Al Batin, Saudi Arabia; ^bElectrical Engineering Department, King Fahd University of Petroleum and Minerals, Dhahran, Saudi Arabia

ABSTRACT

Induction machines have a highly nonlinear model with only partial state information. The unavailability of all states and the presence of unknown disturbances make controller design and proving closed-loop stability challenging tasks. In this paper, we present a control scheme for induction motor speed control using a reduced, second-order model. The model greatly simplifies the control structure and its stability analysis. Current and speed measurements are used while the unknown flux and load torque are estimated using observers. The closed-loop stability of the observer-based control structure is established using Lyapunov's analysis. Simulation studies carried out on a 50 HP induction motor driven by a three-phase inverter show that the proposed controller achieves good speed control for both the regulation and tracking test cases under unknown disturbance.

ARTICLE HISTORY

Received 5 December 2017
Accepted 20 July 2018

KEYWORDS

Induction motor control;
observer-based control;
speed control

1. Introduction

Induction motors (IMs) are widely used in both industrial and household applications. They have a number of desirable features like low cost, ruggedness, spark-free operation, low maintenance requirements and high torque-producing capabilities. Despite these traits, control design for an IM remains a challenge primarily due to two main reasons: (1) nonlinear model and (2) unavailability of complete state information. Therefore, they are still a focus of modern research works dealing with novel, effective and efficient control design methods for the IM.

Field-oriented control (FOC), also referred to as vector control, introduced by Blaschke [1], is a technique for controlling an IM whereby the torque-producing and magnetizing components of the stator currents are decoupled through mathematical transformations, leading to a simplification of the control task, in a manner similar to that of a dc motor. FOC also gives good transient response, making it a suitable method for high-performance IM control [2,3].

The key steps in IM control design are its synthesis and stability assessment. IM control using FOC has been addressed frequently in past research. The reported works include nonlinear control techniques like an input–output feedback linearization [4,5], sliding mode control and sliding mode observers [6,7], adaptive control [8], adaptive sliding mode control [9], backstepping control [10], and also cover methods like stochastic iterative learning control [11], adaptive disturbance rejection control [12] and auto-disturbance

rejection control [13]. The classical proportional plus integral (PI) also continues to be featured in recent works with some variations, like hybrid fuzzy PID [14] and PI control with integral antiwindup [15].

Most of these works use the full fifth-order model for designing control since it captures most of the transient effects and closely approximates the actual machine. Proving closed-loop stability for this full-order model, in the presence of unknown information like flux and load torque, remains a challenge. From this perspective, previous works have some limitations – they either require careful parameter selection for convergence [13], are analytically complex [11], or do not validate the closed-loop stability of the control system [13,14,16]. Some works exist [17] that have proposed simplified models to conveniently capture the transient effects (such as deep-bar and saturation effects) for high power applications. However, the focus of this work is on controlling the speed in steady state. With this in mind, this work aims to simplify the task of controller synthesis and stability analysis by employing a reduced-order model while achieving high performance for steady-state speed control. We show that by neglecting some dynamics, the full-order model is closely approximated by the reduced-order model and the transient effects are averaged out. The presented approach offers a threefold advantage: (1) the speed and flux are directly linked to their individual control variables instead of through intermediate quantities, and hence, can be controlled directly, (2) a simpler control structure is realized as a result of order reduction

and, (3) stability analysis is facilitated by the simpler control structure despite the presence of unknown variables like flux and load torque. Moreover, steady-state performance remains largely unaffected. To establish closed-loop stability is established via developing a generalized version of the results presented in [18] and can now be applied to higher-order systems; another contribution of this work. The scheme herein measurements of current and speed, and estimates of unknown flux and load torque through observers, leading to an observer-based control topology.

2. Modelling

The fifth-order nonlinear IM model in the dq reference frame can be written in the form [19]:

$$\begin{aligned} \dot{x} &= f(x) + g(x)u, \\ y &= h(x), \end{aligned} \quad (1)$$

where the state x , input u and output y are

$$\begin{aligned} x &= [i_{sd} \quad i_{sq} \quad \phi_{rd} \quad \phi_{rq} \quad \Omega]^T, \\ u &= [v_{sd} \quad v_{sq} \quad T_l]^T, \\ y &= [i_{sd} \quad i_{sq} \quad \Omega]^T, \end{aligned} \quad (2)$$

and

$$\begin{aligned} f(x) &= \begin{bmatrix} -\gamma i_{sd} + \omega_s i_{sq} + ba\phi_{rd} + bp\Omega\phi_{rq} + m_1 v_{sd} \\ -\omega_s i_{sd} - \gamma i_{sq} - bp\Omega\phi_{rd} + ba\phi_{rq} + m_1 v_{sq} \\ aM_{sr}i_{sd} - a\phi_{rd} + (\omega_s - p\Omega)\phi_{rq} \\ aM_{sr}i_{sq} - (\omega_s - p\Omega)\phi_{rd} - a\phi_{rq} \\ m(\phi_{rd}i_{sq} - \phi_{rq}i_{sd}) - c\Omega - \frac{T_l}{J} \end{bmatrix}, \\ g(x) &= \begin{bmatrix} m_1 & 0 & 0 \\ 0 & m_1 & 0 \\ 0 & 0 & 0 \\ 0 & 0 & 0 \\ 0 & 0 & -\frac{1}{J} \end{bmatrix}, \quad h(x) = \begin{bmatrix} i_{sd} \\ i_{sq} \\ \Omega \end{bmatrix}. \end{aligned} \quad (3)$$

Here the subscripts (s, r) denote stator and rotor quantities, respectively, subscripts (d, q) denote d -axis and q -axis quantities, ϕ represents flux, i represents current, ω_s denotes stator electrical angular frequency, Ω denotes the rotor mechanical angular speed, p denotes pole-pairs, v denotes voltage input, T_l denotes load torque input and J denotes rotor's moment of inertia. The auxiliary quantities are defined as $a = R_r/L_r$, $b = M_{sr}/\sigma L_s L_r$, $c = f_v/J$, $\gamma = (L_r^2 R_s + M_{sr}^2 R_r)/(\sigma L_s L_r^2)$, $\sigma = 1 - (M_{sr}^2/L_s L_r)$, $m = pM_{sr}/JL_r$, $m_1 = 1/\sigma L_s$ where R denotes resistance, L denotes cyclic inductance, M denotes mutual cyclic inductance, and f_v denotes the viscous friction coefficient.

2.1. Simplified model

The dynamics of current in (1) can be written as

$$\begin{aligned} \sigma \frac{d}{dt} i_{sd} &= -\frac{L_r^2 R_s + M_{sr}^2 R_r}{L_s L_r^2} i_{sd} + \sigma \omega_s i_{sq} + \frac{aM_{sr}}{L_s L_r} \phi_{rd} \\ &\quad + \frac{pM_{sr}}{L_s L_r} \Omega \phi_{rq} + \frac{1}{L_s} v_{sd}, \\ \sigma \frac{d}{dt} i_{sq} &= -\sigma \omega_s i_{sd} - \frac{L_r^2 R_s + M_{sr}^2 R_r}{L_s L_r^2} i_{sq} - \frac{pM_{sr}}{L_s L_r} \Omega \phi_{rd} \\ &\quad + \frac{aM_{sr}}{L_s L_r} \phi_{rq} + \frac{1}{L_s} v_{sq}, \end{aligned} \quad (4)$$

where the equations are multiplied by σ after substituting the values of b , γ and m_1 . The parameter σ is usually small. Therefore, the derivative terms in (4) are small and can be ignored. Moreover, since in the rotating dq frame, the currents become dc quantities in their steady states, ignoring their dynamics does not affect the steady-state response. Thus, the differential equations in (4) reduce to algebraic equations in i_{sd} and i_{sq} . Solving (4) for currents, we get

$$\begin{aligned} i_{sd} &= \frac{1}{\gamma} (\omega_s i_{sq} + ba\phi_{rd} + bp\Omega\phi_{rq} + m_1 v_{sd}), \\ i_{sq} &= \frac{1}{\gamma} (-\omega_s i_{sd} - bp\Omega\phi_{rd} + ba\phi_{rq} + m_1 v_{sq}), \end{aligned} \quad (5)$$

which can be further solved to obtain the currents explicitly as

$$\begin{aligned} i_{sd} &= \left[bp\Omega(\gamma\phi_{rq} - \omega_s\phi_{rd}) + ab(\omega_s\phi_{rq} + \gamma\phi_{rd}) \right. \\ &\quad \left. + m_1(\gamma v_{sd} + \omega_s v_{sq}) \right] \frac{1}{\gamma^2 + \omega_s^2}, \\ i_{sq} &= - \left[bp\Omega(\gamma\phi_{rd} + \omega_s\phi_{rq}) + ab(\omega_s\phi_{rd} - \gamma\phi_{rq}) \right. \\ &\quad \left. + m_1(\omega_s v_{sd} - \gamma v_{sq}) \right] \frac{1}{\gamma^2 + \omega_s^2}. \end{aligned} \quad (6)$$

It follows that the original fifth-order model (1) approximates to a third-order model of the form:

$$\begin{aligned} \dot{x}_r &= f_r(x, u), \\ y_r &= h_r(x) \end{aligned} \quad (7)$$

with

$$\begin{aligned} x_r &= [\phi_{rd} \quad \phi_{rq} \quad \Omega]^T, \\ u &= [v_{sd} \quad v_{sq} \quad T_l]^T, \\ y_r &= \Omega. \end{aligned} \quad (8)$$

The expression for $f_r(x, u)$ can be derived by substituting (6) into (1). Simulations were run to illustrate the comparison between models (1) and (7) on an IM whose parameters are given in Table 1 taken from [3]. Rated three-phase voltages were applied to the

Table 1. Parameters of the IM.

Nominal power	50 HP
Nominal angular speed	1780 rpm
No. of pole-pairs	2
Nominal voltage (line-line)	460 V
R_s	0.087 Ω
R_r	0.228 Ω
L_s	0.0355 H
L_r	0.0355 H
M_{sr}	0.0347 H
J	1.662 kg m ²
f_v	0.1 N m s ⁻¹

IM with rated load of 200 N m applied at $t = 1$ s in open-loop configuration. Speed and electromagnetic torque T_e responses are depicted in Figure 1 while the current responses are shown in Figure 2. Three-phase quantities were converted to dq reference frame using the transformation reported in [18] and T_e was calculated as

$$T_e = pM_{sr}\phi_{rd}i_{sq} \quad (9)$$

for both models. The plots indicate that (7) closely approximates (1), with the reduced model states acting as average estimates of the original model in the transient regime.

3. Field-oriented feedback linearizing control

3.1. Controller design

In FOC, the synchronous reference frame is chosen such that all the flux lies along the d -axis with $\phi_{rq} = 0$. It can be shown from (1) that this can be achieved by

choosing ω_s as

$$\omega_s = p\Omega + \frac{aM_{sr}}{\phi_{rd}}i_{sq}, \quad (10)$$

and achieving “field orientation” with $\phi_{rq} = 0$, $\dot{\phi}_{rq} = 0$. Consequently, the third-order model (7) reduces by another order, and can be written as

$$\begin{aligned} \frac{d}{dt}\phi_{rd} &= aM_{sr}i_{sd} - a\phi_{rd}, \\ \frac{d}{dt}\Omega &= m\phi_{rd}i_{sq} - c\Omega - \frac{T_l}{J}, \end{aligned} \quad (11)$$

where

$$\begin{aligned} i_{sd} &= \frac{1}{\gamma}(\omega_s i_{sq} + ba\phi_{rd} + m_1 v_{sd}), \\ i_{sq} &= \frac{1}{\gamma}(-\omega_s i_{sd} - bp\Omega\phi_{rd} + m_1 v_{sq}), \end{aligned} \quad (12)$$

follow from putting $\phi_{rq} = 0$ in (5). Substitution of (12) into (11) leads to the final second-order model utilized for control design:

$$\begin{aligned} \frac{d}{dt}\phi_{rd} &= \frac{aM_{sr}}{\gamma}(\omega_s i_{sq} + ba\phi_{rd} + m_1 v_{sd}) - a\phi_{rd}, \\ \frac{d}{dt}\Omega &= \frac{m\phi_{rd}}{\gamma}(-\omega_s i_{sd} - bp\Omega\phi_{rd} + m_1 v_{sq}) \\ &\quad - c\Omega - \frac{T_l}{J}. \end{aligned} \quad (13)$$

Remark 3.1: Notice that flux dynamics $\dot{\phi}_{rd}$ in (13) are completely independent from speed dynamics $\dot{\Omega}$, and

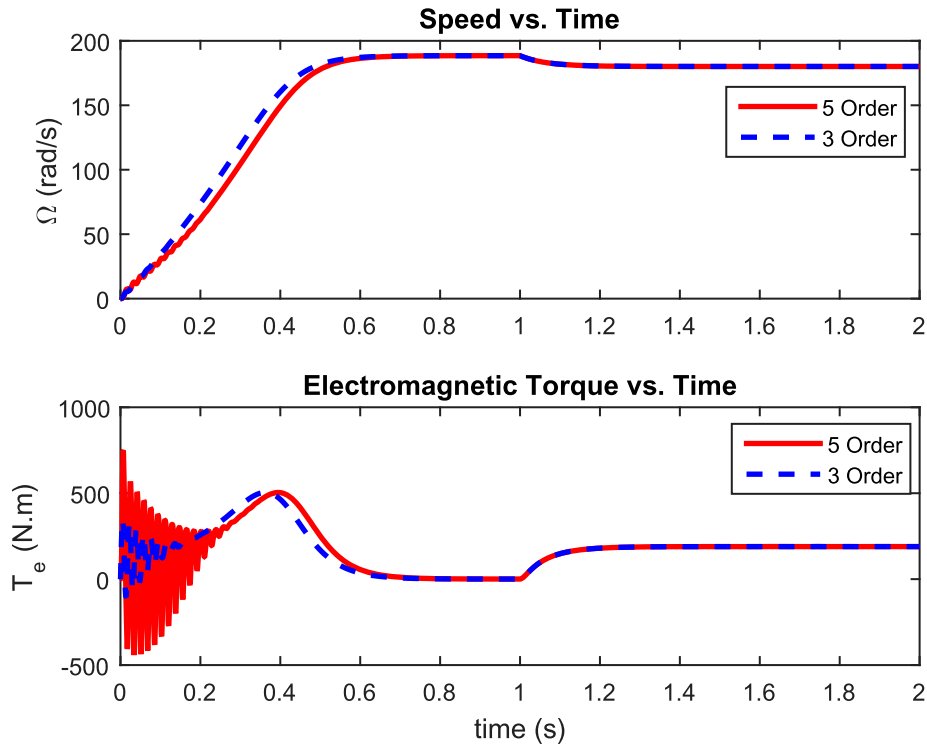


Figure 1. Open-loop speed and torque comparison.

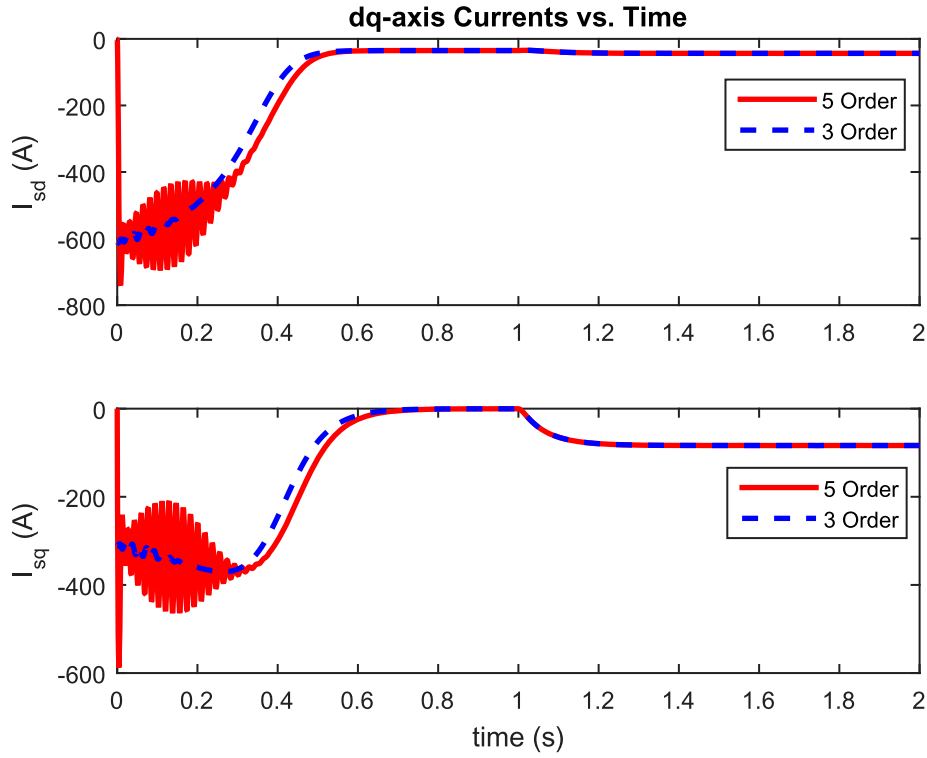


Figure 2. Open-loop current comparison.

with current measurements readily available, flux ϕ_{rd} can be directly controlled from the voltage input v_{sd} . Similarly, speed Ω can now be controlled from the voltage input v_{sq} . In other words, the model links the variables to be controlled i.e. ϕ_{rd} and Ω , directly to the control variables v_{sd} and v_{sq} , respectively. In contrast, when using the full-order model of (1), it is often required that flux and speed must first be controlled through intermediate variables, namely currents, which must then be regulated to certain references as required by flux and speed control, through the voltages (e.g. backstepping control, see [10,19]). This multistep approach leads to a complex control law, whose stability analysis is further complicated by unknown quantities like flux and load torque. Thus, the simplification achieved by the model (13) makes the task of controller design easier and also facilitates stability analysis.

Let us define new error quantities as

$$\begin{aligned} e_\phi &= \phi_{rd} - \phi^*, \\ \tilde{e}_\phi &= \phi_{rd} - \hat{\phi}, \\ \bar{e}_\phi &= \hat{\phi} - \phi^*, \\ e_\Omega &= \Omega - \Omega^*, \\ \tilde{e}_T &= T_l - \hat{T}_l, \end{aligned} \quad (14)$$

where ϕ^* is the reference flux for ϕ_{rd} , $\hat{\phi}$ is its estimate (both in Wb), Ω^* is the reference speed in rad/s, and \hat{T}_l is the load torque estimate in N m. The dynamics of the flux error e_ϕ and the speed error e_Ω can be written

using (13) and (14) as

$$\begin{aligned} \dot{e}_\phi &= \frac{aM_{sr}}{\gamma} (\omega_s i_{sq} + ba\phi_{rd} + m_1 v_{sd}) - a\phi_{rd} - \dot{\phi}^*, \\ \dot{e}_\Omega &= \frac{m\phi_{rd}}{\gamma} (-\omega_s i_{sd} - bp\Omega\phi_{rd} + m_1 v_{sq}) \\ &\quad - c\Omega - \frac{T_l}{J} - \dot{\Omega}^*. \end{aligned} \quad (15)$$

Selecting v_{sd} and v_{sq} in (15) as

$$\begin{aligned} v_{sd} &= \frac{1}{m_1} \left(\frac{\gamma}{M_{sr}} - ba \right) \phi^* \quad \text{for } i_{sd} = 0, \\ v_{sd} &= \frac{1}{m_1} \left[-\hat{\omega}_s i_{sq} - ba\hat{\phi} + \frac{\gamma}{M_{sr}} \hat{\phi} \right. \\ &\quad \left. + \frac{\gamma}{aM_{sr}} (\dot{\phi}^* - K_\phi \bar{e}_\phi) \right] \quad \text{for } i_{sd} \neq 0, \\ v_{sq} &= \frac{1}{m_1} \left[\hat{\omega}_s i_{sd} + bp\Omega\hat{\phi} \right. \\ &\quad \left. + \frac{\gamma}{m\hat{\phi}} \left(c\Omega + \frac{\hat{T}_l}{J} + \dot{\Omega}^* - K_\Omega e_\Omega \right) \right], \end{aligned} \quad (16)$$

with K_ϕ and K_Ω as positive constants to be selected, and $\hat{\omega}_s$ estimated as

$$\hat{\omega}_s = \frac{aM_{sr}i_{sq}}{\hat{\phi}} + p\Omega, \quad (17)$$

we get

$$\begin{aligned}\dot{e}_\phi &= -K_\phi \bar{e}_\phi + \frac{aM_{sr}i_{sq}}{\gamma}(\omega_s - \hat{\omega}_s) \\ &\quad + \left(\frac{ba^2M_{sr}}{\gamma} - a \right) \tilde{e}_\phi, \\ \dot{e}_\Omega &= -\frac{m\phi_{rd}i_{sd}}{\gamma}(\omega_s - \hat{\omega}_s) - \frac{bpm}{\gamma}\Omega\phi_{rd}\tilde{e}_\phi \\ &\quad + \frac{\phi_{rd}}{\hat{\phi}} \left(c\Omega + \frac{\hat{T}_l}{J} - K_\Omega e_\Omega + \dot{\Omega}^* \right) \\ &\quad - c\Omega - \frac{T_l}{J} - \dot{\Omega}^*.\end{aligned}\quad (18)$$

From the first three equations in (14), we can write

$$\begin{aligned}\frac{\phi_{rd}}{\hat{\phi}} &= \tilde{e}_\phi + 1, \\ \bar{e}_\phi &= e_\phi - \tilde{e}_\phi.\end{aligned}\quad (19)$$

From (10), (17) and (14), we get

$$\begin{aligned}\omega_s - \hat{\omega}_s &= aM_{sr}i_{sq} \left(\frac{1}{\phi_{rd}} - \frac{1}{\hat{\phi}} \right), \\ &= -\frac{aM_{sr}i_{sq}}{\phi_{rd}\hat{\phi}}(\phi_{rd} - \hat{\phi}), \\ &= -\frac{aM_{sr}i_{sq}}{\phi_{rd}\hat{\phi}}\tilde{e}_\phi.\end{aligned}\quad (20)$$

Substitution of (19) and (20) in (18) leads to

$$\begin{aligned}\dot{e}_\phi &= -K_\phi e_\phi + \left(\frac{ba^2M_{sr}}{\gamma} - a + K_\phi \right. \\ &\quad \left. - \frac{a^2M_{sr}^2}{\gamma} \frac{i_{sq}^2}{\phi_{rd}\hat{\phi}} \right) \tilde{e}_\phi, \\ \dot{e}_\Omega &= -K_\Omega e_\Omega + \left(\frac{maM_{sr}}{\gamma} \frac{i_{sd}i_{sq}}{\hat{\phi}} - \frac{bpm}{\gamma}\Omega\phi_{rd} \right. \\ &\quad \left. + c\Omega + \frac{\hat{T}_l}{J} - K_\Omega e_\Omega + \dot{\Omega}^* \right) \tilde{e}_\phi - \frac{\tilde{e}_T}{J}.\end{aligned}\quad (21)$$

3.2. Observer design

Both the rotor flux and load torque are estimated using first-order exponential observers. Let the dynamics of the rotor flux estimate $\hat{\phi}$ be

$$\dot{\hat{\phi}} = aM_{sr}i_{sd} - a\hat{\phi}. \quad (22)$$

Subtracting (22) from the first equation of (11), we get

$$\dot{\tilde{e}}_\phi = -a\tilde{e}_\phi, \quad (23)$$

which indicates that \tilde{e}_ϕ will exponentially converge to zero. For the load torque observer, we define new variables z and \hat{z} such that [18]

$$\begin{aligned}z &= T_l + K_T\Omega, \\ \hat{z} &= \hat{T}_l + K_T\Omega,\end{aligned}\quad (24)$$

where K_T is a positive constant to be selected. Assume

$$\dot{\hat{T}}_l = 0. \quad (25)$$

Recall the second equation from model (11);

$$\frac{d}{dt}\Omega = m\phi_{rd}i_{sq} - c\Omega - \frac{T_l}{J}. \quad (26)$$

The dynamical equations of z in (24) can be written using model (11) as

$$\begin{aligned}\dot{z} &= \dot{\hat{T}}_l + K_T\dot{\Omega} \\ &= mK_T\phi_{rd}i_{sq} + \left(\frac{K_T^2}{J} - cK_T \right) \Omega - \frac{K_T}{J}z.\end{aligned}\quad (27)$$

Let \hat{z} be calculated through

$$\dot{\hat{z}} = -\frac{K_T}{J}\hat{z} + \left(\frac{K_T^2}{J} - cK_T \right) \Omega + mK_T\hat{\phi}i_{sq}, \quad (28)$$

$$\hat{z}(0) = \hat{T}_l(0) + K_T\Omega(0).$$

\hat{T}_L can be estimated from \hat{z} as

$$\hat{T}_L = \hat{z} - K_T\Omega. \quad (29)$$

Defining

$$\tilde{e}_z = z - \hat{z}, \quad (30)$$

we can write

$$\dot{\tilde{e}}_z = -\frac{K_T}{J}\tilde{e}_z + mK_Ti_{sq}\tilde{e}_\phi. \quad (31)$$

It follows from (24) that

$$\tilde{e}_T = \tilde{e}_z. \quad (32)$$

Block diagram of flux and load torque observers is shown in Figure 3 while that of the IM drive under closed-loop control is shown in Figure 4.

3.3. Stability analysis

To assess the stability of the observer-based closed-loop control, we develop a generalized version of Lemma A.1 in [18] and apply it to the error dynamics.

Lemma 3.1: *Given the system*

$$\begin{aligned}\dot{x}_1 &= f_1(t, x), \\ \dot{x}_2 &= f_2(t, x), \\ &\vdots \\ \dot{x}_{n-1} &= f_{n-1}(t, x), \\ \dot{x}_n &= f_n(t, x),\end{aligned}\quad (33)$$

with $x \in \mathbb{R}^n$, $f_i(t, 0) = 0$, $i = 1, 2, \dots, n$.

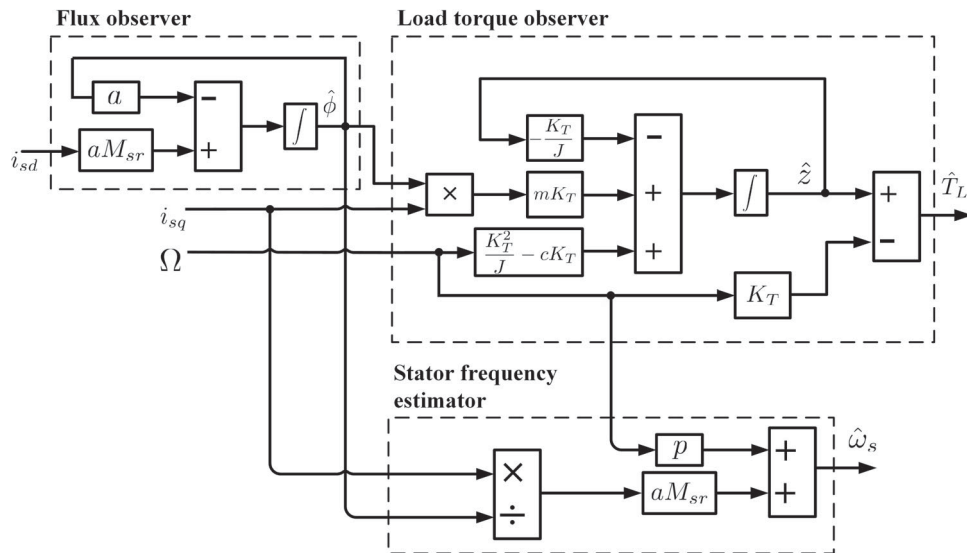


Figure 3. Block diagram of flux and load torque observers.

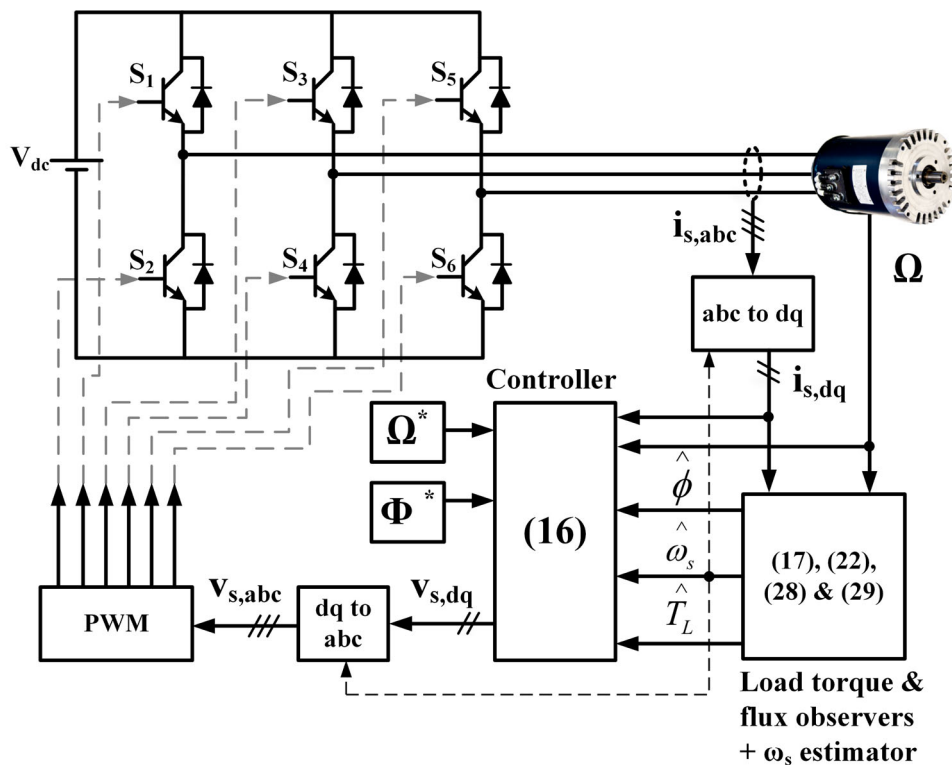


Figure 4. Block diagram of closed-loop control.

Assumption 1: for the subsystems in (33) defined by dynamics $\dot{x}_1, \dot{x}_2, \dots, \dot{x}_{n-1}$, let there exist functions $V_1(t, x_1), V_2(t, x_2), \dots, V_{n-1}(t, x_{n-1})$ such that

$$\begin{aligned} c_{1,1}\|x_1\|^2 &\leq V_1(t, x_1) \leq c_{2,1}\|x_1\|^2, \\ c_{1,2}\|x_2\|^2 &\leq V_2(t, x_2) \leq c_{2,2}\|x_2\|^2, \\ &\vdots \\ c_{1,n-1}\|x_{n-1}\|^2 &\leq V_{n-1}(t, x_{n-1}) \leq c_{2,n-1}\|x_{n-1}\|^2, \end{aligned} \quad (34)$$

with $c_{i,j} > 0$, $i, j = 1, 2, \dots, n-1$, and

$$\begin{aligned} \frac{\partial V_1}{\partial t} + \frac{\partial V_1}{\partial x_1} f_1(t, x) &\leq -k_{1,1}\|x_1\|^2 - k_{1,2}\|x_2\|^2 \\ &\quad - \dots - k_{1,n-1}\|x_{n-1}\|^2 + k_{1,n}\|x_n\|^2, \\ \frac{\partial V_2}{\partial t} + \frac{\partial V_2}{\partial x_2} f_2(t, x) &\leq -k_{2,1}\|x_1\|^2 - k_{2,2}\|x_2\|^2 \\ &\quad - \dots - k_{2,n-1}\|x_{n-1}\|^2 + k_{2,n}\|x_n\|^2, \\ &\vdots \end{aligned}$$

$$\begin{aligned} \frac{\partial V_{n-1}}{\partial t} + \frac{\partial V_{n-1}}{\partial x_{n-1}} f_{n-1}(t, x) &\leq -k_{n-1,1} \|x_1\|^2 \\ &\quad - k_{n-1,2} \|x_2\|^2 - \dots - k_{n-1,n-1} \|x_{n-1}\|^2 \\ &\quad + k_{n-1,n} \|x_n\|^2, \end{aligned} \tag{35}$$

with $k_{i,j} > 0$, $i, j = 1, 2, \dots, n - 1$, and $k_{i,j} \geq 0$, $i = 1, 2, \dots, n - 1$, $j = n$.

Assumption 2: the equilibrium point $x_n = 0$ of the subsystem \dot{x}_n is globally exponentially stable.

Then, the equilibrium point $x = 0$ of the whole system (33) is globally exponentially stable.

Proof: By assumption 2 on subsystem \dot{x}_n , for any initial condition $x_n(t_0)$, $x_n(t)$ fulfils the inequality

$$\|x_n(t)\| \leq c_3 \|x_n(t_0)\| e^{-c_4(t-t_0)}, \tag{36}$$

for some constants $c_3 > 0$ and $c_4 > 0$. Let $z(t) \in \mathbb{R}$ be the solution of

$$\dot{z}(t) = -c_4 z(t), \quad z(t_0) = \|x_n(t_0)\|. \tag{37}$$

Since $z(t) = z(t_0)e^{-c_4(t-t_0)}$, we can write

$$\|x_n(t)\| \leq c_3 z(t), \quad \forall t \geq t_0. \tag{38}$$

Define a function $V(t, x_1, x_2, \dots, x_{n-1}, z)$ as

$$\begin{aligned} V(t, x_1, x_2, \dots, x_{n-1}, z) &= V_1(t, x_1) + V_2(t, x_2) \\ &\quad + \dots + V_{n-1}(t, x_{n-1}) + \frac{1}{2}(k_{1,n} + 1) \frac{c_3^2}{c_4} z^2 \\ &\quad + \frac{1}{2}(k_{2,n} + 1) \frac{c_3^2}{c_4} z^2 + \dots + \frac{1}{2}(k_{n-1,n} + 1) \frac{c_3^2}{c_4} z^2 \\ &= \sum_{j=1}^{n-1} \left(V_j(t, x_j) + \frac{1}{2}(k_{j,n} + 1) \frac{c_3^2}{c_4} z^2 \right). \end{aligned} \tag{39}$$

Owing to (34), we have, for every $t \geq t_0$

$$\begin{aligned} c_{1,1} \|x_1\|^2 + c_{1,2} \|x_2\|^2 + \dots + c_{1,n-1} \|x_{n-1}\|^2 \\ + \sum_{j=1}^{n-1} \left(\frac{1}{2}(k_{j,n} + 1) \frac{c_3^2}{c_4} z^2 \right) \leq V \leq c_{2,1} \|x_1\|^2 \\ + c_{2,2} \|x_2\|^2 + \dots + c_{2,n-1} \|x_{n-1}\|^2 \\ + \sum_{j=1}^{n-1} \left(\frac{1}{2}(k_{j,n} + 1) \frac{c_3^2}{c_4} z^2 \right), \end{aligned} \tag{40}$$

which can be written more compactly as

$$\begin{aligned} \sum_{j=1}^{n-1} \left(c_{1,j} \|x_j\|^2 + \frac{1}{2}(k_{j,n} + 1) \frac{c_3^2}{c_4} z^2 \right) \leq V \\ \leq \sum_{j=1}^{n-1} \left(c_{2,j} \|x_j\|^2 + \frac{1}{2}(k_{j,n} + 1) \frac{c_3^2}{c_4} z^2 \right). \end{aligned} \tag{41}$$

Differentiating (39) to get \dot{V} gives

$$\begin{aligned} \dot{V} &= \sum_{j=1}^{n-1} (\dot{V}_j(t, x_j) - (k_{j,n} + 1) c_3^2 z^2) \\ &= \sum_{j=1}^{n-1} \left(\frac{\partial V_j}{\partial t} + \frac{\partial V_j}{\partial x_i} f_i(t, x) - (k_{j,n} + 1) c_3^2 z^2 \right). \end{aligned} \tag{42}$$

By virtue of (35), we have, for every $t \geq t_0$

$$\begin{aligned} \dot{V} &\leq \sum_{j=1}^{n-1} (-k_{j,1} \|x_1\|^2 - k_{j,2} \|x_2\|^2 - \dots - k_{j,n-1} \\ &\quad \|x_{n-1}\|^2 + k_{j,n} \|x_n\|^2 - k_{j,n} c_3^2 z^2) - c_3^2 z^2, \end{aligned} \tag{43}$$

or, more precisely as

$$\begin{aligned} \dot{V} &\leq - \sum_{j=1}^{n-1} \sum_{i=1}^{n-1} k_{i,j} \|x_j\|^2 \\ &\quad + \sum_{j=1}^{n-1} (k_{j,n} \|x_n\|^2 - k_{j,n} c_3^2 z^2) - c_3^2 z^2. \end{aligned} \tag{44}$$

By (38), we get

$$\dot{V} \leq - \sum_{i=1}^{n-1} \sum_{j=1}^{n-1} k_{i,j} \|x_j\|^2 - c_3^2 z^2 \leq 0. \tag{45}$$

■

The results of Lemma 3.1 can be applied to the error dynamics to show their exponential convergence to zero. Rewriting the error dynamics from (21), (23) and (31) and replacing \tilde{e}_z with \tilde{e}_T as per (32) gives

$$\begin{aligned} \dot{e}_\phi &= -K_\phi e_\phi + \left(\frac{ba^2 M_{sr}}{\gamma} - a + K_\phi \right. \\ &\quad \left. - \frac{a^2 M_{sr}^2}{\gamma} \frac{i_{sq}^2}{\phi_{rd} \hat{\phi}} \right) \tilde{e}_\phi, \\ \dot{e}_\Omega &= -K_\Omega e_\Omega + \left(\frac{ma M_{sr}}{\gamma} \frac{i_{sd} i_{sq}}{\hat{\phi}} - \frac{bpm}{\gamma} \Omega \phi_{rd} \right. \\ &\quad \left. + c\Omega + \frac{\hat{T}_l}{J} - K_\Omega e_\Omega + \dot{\Omega}^* \right) \tilde{e}_\phi - \frac{\tilde{e}_T}{J}, \\ \dot{\tilde{e}}_T &= -\frac{K_T}{J} \tilde{e}_T + mK_T i_{sq} \tilde{e}_\phi, \\ \dot{\tilde{e}}_\phi &= -a\tilde{e}_\phi. \end{aligned} \tag{46}$$

Let

$$x = \begin{bmatrix} x_1 \\ x_2 \\ x_3 \\ x_4 \end{bmatrix} = \begin{bmatrix} e_\phi \\ e_\Omega \\ \tilde{e}_T \\ \tilde{e}_\phi \end{bmatrix}, \tag{47}$$

and

$$\begin{aligned}\xi_1 &= \frac{ba^2M_{sr}}{\gamma} - a + K_\phi - \frac{a^2M_{sr}^2}{\gamma} \frac{i_{sq}^2}{\phi_{rd}\hat{\phi}}, \\ \xi_2 &= \frac{maM_{sr}}{\gamma} \frac{i_{sd}i_{sq}}{\hat{\phi}} - \frac{bpm}{\gamma} \Omega\phi_{rd} + c\Omega + \frac{\hat{T}_l}{J} \\ &\quad - K_\Omega x_2 + \dot{\Omega}^*, \\ \xi_3 &= mK_T i_{sq}.\end{aligned}\quad (48)$$

We can write system (46) as

$$\begin{aligned}\dot{x}_1 &= -K_\phi x_1 + \xi_1 x_4, \\ \dot{x}_2 &= -K_\Omega x_2 - \frac{1}{J} x_3 + \xi_2 x_4, \\ \dot{x}_3 &= -\frac{K_T}{J} x_3 + \xi_3 x_4, \\ \dot{x}_4 &= -ax_4.\end{aligned}\quad (49)$$

Clearly, x_4 is globally exponentially stable, satisfying assumption 2 of Lemma 3.1. Define functions

$$\begin{aligned}V_1 &= \frac{1}{2}x_1^2, \\ V_2 &= \frac{1}{2}x_2^2, \\ V_3 &= \frac{1}{2}x_3^2,\end{aligned}\quad (50)$$

and

$$V = V_1 + V_2 + V_3 = \frac{1}{2}(x_1^2 + x_2^2 + x_3^2).\quad (51)$$

Clearly,

$$\begin{aligned}\frac{1}{4}x_1^2 &\leq V_1 \leq x_1^2, \\ \frac{1}{4}x_2^2 &\leq V_2 \leq x_2^2, \\ \frac{1}{4}x_3^2 &\leq V_3 \leq x_3^2.\end{aligned}\quad (52)$$

Thus, V_i , $i = 1, 2, 3$ fulfil the first condition in assumption 1 in Lemma 3.1. Differentiating (51) gives

$$\begin{aligned}\dot{V} &= \dot{V}_1 + \dot{V}_2 + \dot{V}_3 \\ &= x_1\dot{x}_1 + x_2\dot{x}_2 + x_3\dot{x}_3 \\ &= -K_\phi x_1^2 - K_\Omega x_2^2 - \frac{K_T}{J} x_3^2 + \xi_1 x_1 x_4 \\ &\quad - \frac{1}{J} x_2 x_3 + \xi_2 x_2 x_4 + \xi_3 x_3 x_4.\end{aligned}\quad (53)$$

The last four terms in (53) can be bounded using Cauchy inequality with ε which states that

$$ab \leq \frac{a^2}{2\varepsilon} + \frac{\varepsilon b^2}{2}, \quad \forall a, b \in \mathbb{R}, \forall \varepsilon > 0.\quad (54)$$

It then follows that

$$\begin{aligned}\xi_1 x_1 x_4 &\leq \xi_{1b} \left(\frac{x_1^2}{2\varepsilon_1} + \frac{\varepsilon_1 x_4^2}{2} \right), \\ \frac{1}{J} x_2 x_3 &\leq \frac{1}{J} \left(\frac{x_2^2}{2\varepsilon_2} + \frac{\varepsilon_2 x_3^2}{2} \right), \\ \xi_2 x_2 x_4 &\leq \xi_{2b} \left(\frac{x_2^2}{2\varepsilon_3} + \frac{\varepsilon_3 x_4^2}{2} \right), \\ \xi_3 x_3 x_4 &\leq \xi_{3b} \left(\frac{x_3^2}{2\varepsilon_4} + \frac{\varepsilon_4 x_4^2}{2} \right)\end{aligned}\quad (55)$$

holds $\forall \varepsilon_i > 0$, $i = 1, 2, 3, 4$, where

$$\begin{aligned}\xi_{1b} &= \frac{ba^2M_{sr}}{\gamma} + a + K_\phi \\ &\quad + \frac{a^2M_{sr}^2}{\gamma} \frac{i_{sq,\max}^2}{|\phi_{rd,\min}| \cdot |\hat{\phi}_{\min}|}, \\ \xi_{2b} &= \frac{maM_{sr}}{\gamma} \frac{|i_{sd,\max}| \cdot |i_{sq,\max}|}{|\hat{\phi}_{\min}|} \\ &\quad + \frac{bpm}{\gamma} |\Omega_{\max}| \cdot |\phi_{rd,\max}| + c |\Omega_{\max}| \\ &\quad + \frac{|\hat{T}_{l,\max}|}{J} + K_\Omega |x_{2,\max}| + |\dot{\Omega}_{\max}^*|, \\ \xi_{3b} &= mK_T |i_{sq,\max}|.\end{aligned}\quad (56)$$

Hence, we can write

$$\begin{aligned}\dot{V} &\leq -K_\phi x_1^2 - K_\Omega x_2^2 - \frac{K_T}{J} x_3^2 + \xi_{1b} \left(\frac{x_1^2}{2\varepsilon_1} + \frac{\varepsilon_1 x_4^2}{2} \right) \\ &\quad + \frac{1}{J} \left(\frac{x_2^2}{2\varepsilon_2} + \frac{\varepsilon_2 x_3^2}{2} \right) + \xi_{2b} \left(\frac{x_2^2}{2\varepsilon_3} + \frac{\varepsilon_3 x_4^2}{2} \right) \\ &\quad + \xi_{3b} \left(\frac{x_3^2}{2\varepsilon_4} + \frac{\varepsilon_4 x_4^2}{2} \right).\end{aligned}\quad (57)$$

Collecting the terms, we get

$$\begin{aligned}\dot{V} &\leq \left(-K_\phi + \frac{\xi_{1b}}{2\varepsilon_1} \right) x_1^2 + \left(-K_\Omega + \frac{1}{2J\varepsilon_2} + \frac{\xi_{2b}}{2\varepsilon_3} \right) x_2^2 \\ &\quad + \left(-\frac{K_T}{J} + \frac{\varepsilon_2}{2J} + \frac{\xi_{3b}}{2\varepsilon_4} \right) x_3^2 \\ &\quad + \left(\frac{\xi_{1b}\varepsilon_1}{2} + \frac{\xi_{2b}\varepsilon_3}{2} + \frac{\xi_{3b}\varepsilon_4}{2} \right) x_4^2,\end{aligned}\quad (58)$$

or

$$\begin{aligned}\dot{V} &\leq - \left(K_\phi - \frac{\xi_{1b}}{2\varepsilon_1} \right) \|x_1\|^2 \\ &\quad - \left(K_\Omega - \frac{1}{2J\varepsilon_2} - \frac{\xi_{2b}}{2\varepsilon_3} \right) \|x_2\|^2 \\ &\quad - \left(\frac{K_T}{J} - \frac{\varepsilon_2}{2J} - \frac{\xi_{3b}}{2\varepsilon_4} \right) \|x_3\|^2 \\ &\quad + \left(\frac{\xi_{1b}\varepsilon_1}{2} + \frac{\xi_{2b}\varepsilon_3}{2} + \frac{\xi_{3b}\varepsilon_4}{2} \right) \|x_4\|^2,\end{aligned}\quad (59)$$

or

$$\dot{V} \leq -\alpha_1 \|x_1\|^2 - \alpha_2 \|x_2\|^2 - \alpha_3 \|x_3\|^2 + \alpha_4 \|x_4\|^2, \quad (60)$$

where

$$\begin{aligned} \alpha_1 &= K_\phi - \frac{\xi_{1b}}{2\varepsilon_1}, \\ \alpha_2 &= K_\Omega - \frac{1}{2J\varepsilon_2} - \frac{\xi_{2b}}{2\varepsilon_3}, \\ \alpha_3 &= \frac{K_T}{J} - \frac{\varepsilon_2}{2J} - \frac{\xi_{3b}}{2\varepsilon_4}, \\ \alpha_4 &= \frac{\xi_{1b}\varepsilon_1}{2} + \frac{\xi_{2b}\varepsilon_3}{2} + \frac{\xi_{3b}\varepsilon_4}{2}. \end{aligned} \quad (61)$$

It is clear that $\alpha_4 \geq 0$. Since all the parameters and signals in ξ_{ib} , $i = 1, 2, 3$ are finite and bounded on $[0, \infty)$, the gains K_ϕ , K_Ω and K_T can be conveniently selected with appropriate positive scalars ε_i , $i = 1, 2, 3, 4$ to guarantee $\alpha_i > 0$, $i = 1, 2, 3$. Consequently, the second condition in assumption 1 of Lemma 3.1 is met and the tracking errors of (49) will exponentially converge to zero.

4. Simulation results and discussion

The controller was tested on the speed control of a 50 HP IM driven by a three-phase inverter, and taking detailed inverter switching into account. The motor parameters are given in Table 1. Two simulations test cases were run for 1 s each: the first with a constant speed reference of 120 rad/s with a rated load of

200 N m applied at 0.5 s, and the second with a changing speed reference, stepping up from 120 to 160 rad/s at 0.25 s, then back down to 120 rad/s at 0.75 s, and rated load applied at 0.5 s. Flux reference for both test cases was set to $\phi^* = 0.96$ Wb. The results are shown in Figures 5–8.

From Figure 5 it can be seen that the controller exhibits a fast transient response for both speed regulation and tracking test cases. The actual speed attains its reference within 0.2 s for both tests. As the load torque disturbance is applied, the speed does not get affected much as the control effort causes the electromagnetic torque T_e to increase instantly to counter the load disturbance effects, as seen in Figure 6. The corresponding flux and torque estimation plots in Figures 7 and 8 also show the exponential tracking of reference flux and actual load torque by their respective observers, with the estimated quantities converging to their corresponding references in less than 0.2 s. In summary, the observer-based controller exhibits good transient and steady-state characteristics for both the speed regulation and tracking scenarios.

4.1. Comparison with PI control

The results of the proposed reduced-order control scheme were compared with the conventional PI control to validate its performance. Two PI controllers were used; one for flux regulation using v_{sd} and the other for speed regulation using v_{sq} . Simulations were run using the first test case described previously to compare speed regulation performance. Speed and flux responses are

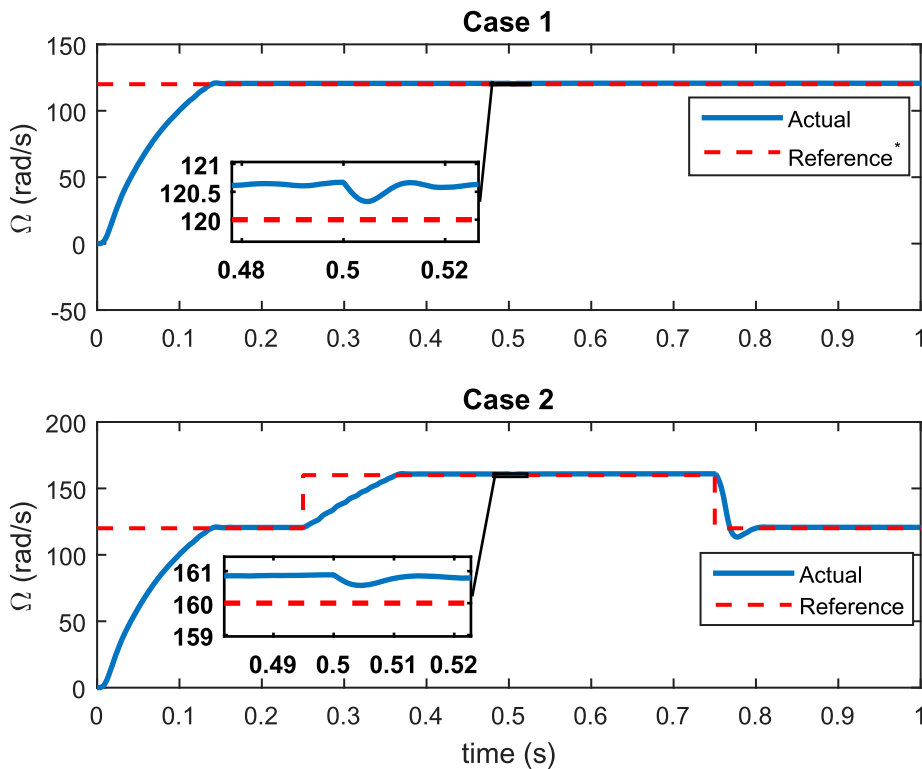


Figure 5. Speed regulation and tracking response, rated load applied at 0.5 s.

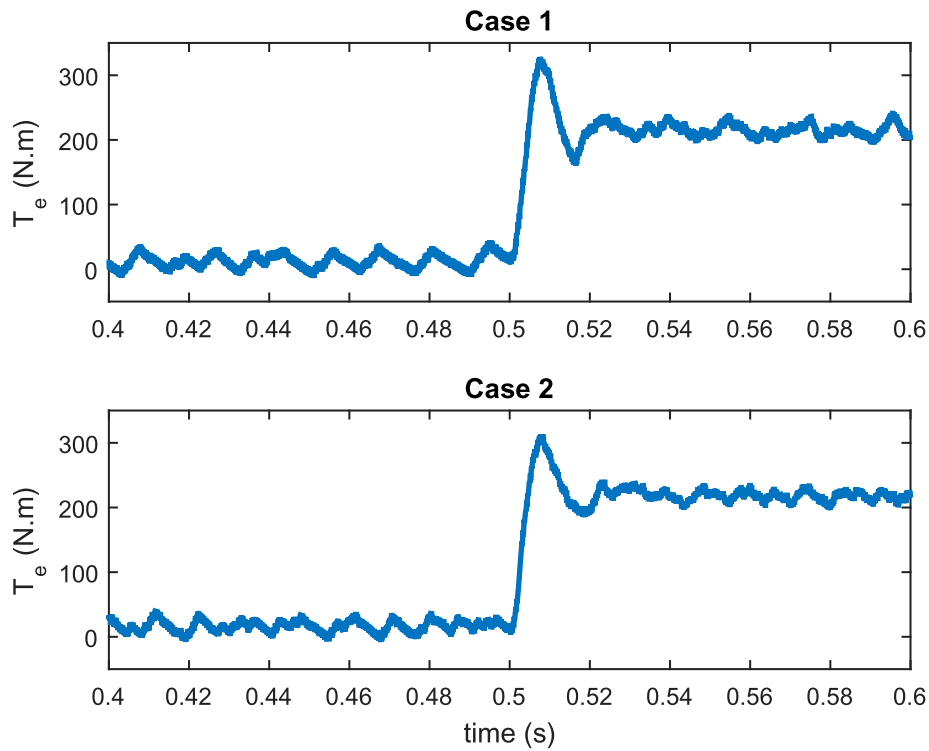


Figure 6. Electromagnetic torque response before and after load application.

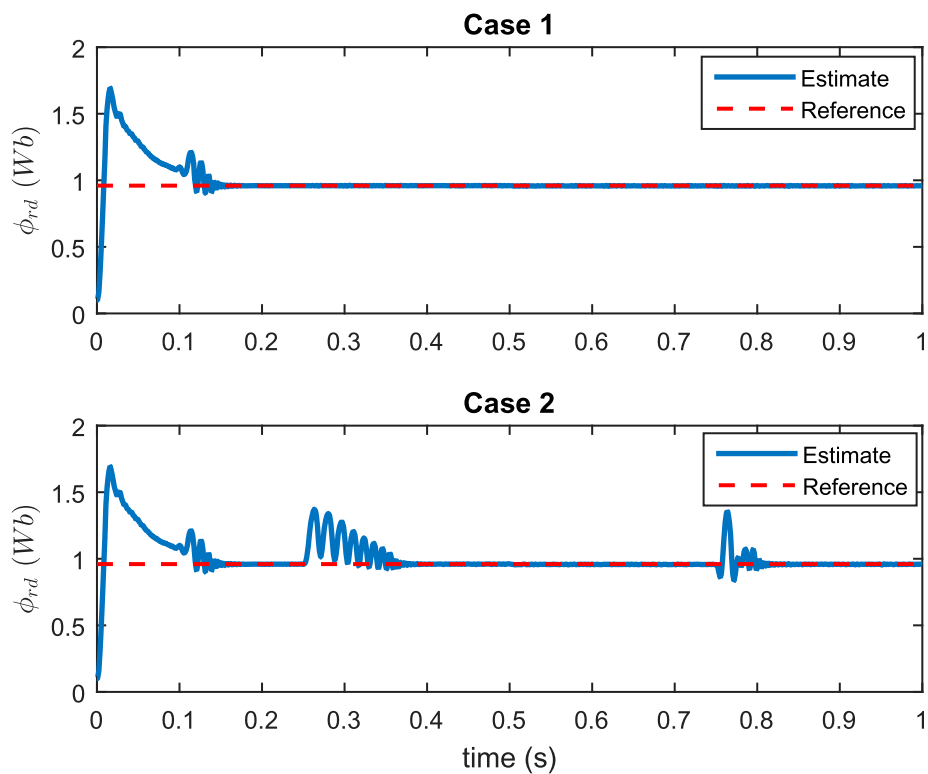


Figure 7. Flux reference and its estimate's response.

plotted in Figure 9. The results indicate that while the speed regulation performance was comparable for the two schemes, the PI controller exhibited poorer flux regulation performance. The flux observer's performance deteriorated under the PI controller due to its weaker regulation response. The proposed scheme, being model-based, performed well in the transient and

steady-state regimes despite ignoring some dynamics. On the other hand, the PI controller did not rely on the model and hence a large overshoot in flux's transient trajectory was observed. The flux response also shows that under PI control, it took longer for the flux to converge to its reference after applying the load disturbance.

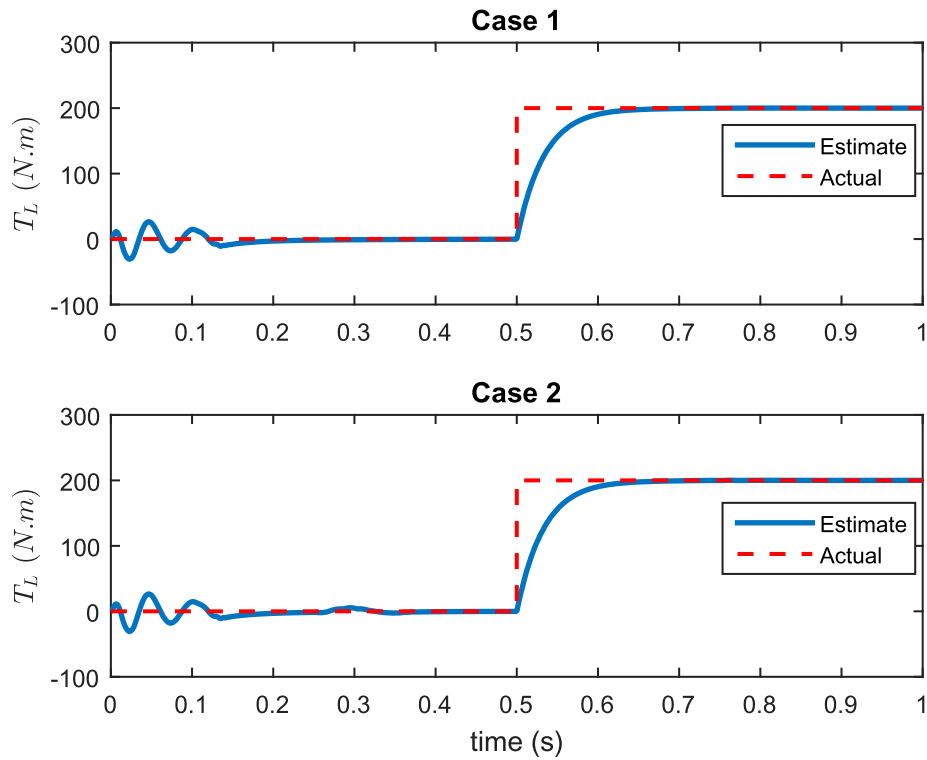


Figure 8. Actual load torque and its estimate's response.

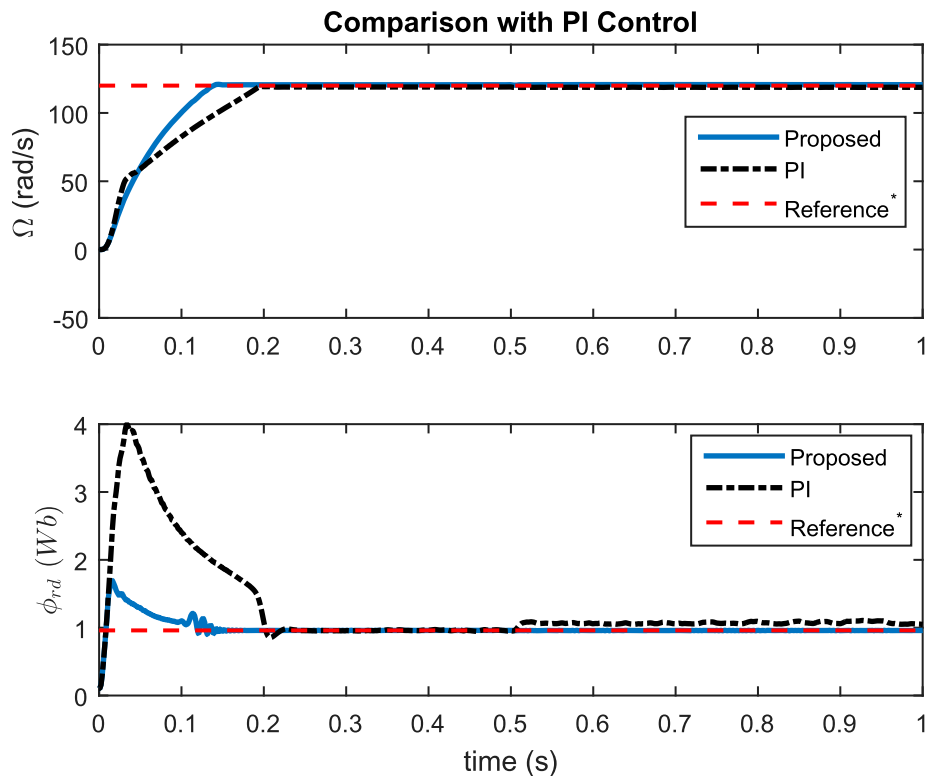


Figure 9. Comparison with PI control.

5. Conclusion

In this paper, we have developed a simple technique for IM speed control using a reduced-order model. It is first shown that the lower-order model approximates the original one with sufficient accuracy. When field orientation is applied to this model, apart from the inherent

decoupling of FOC, it also yields a direct relationship between the variables to be controlled and the input quantities. This not only leads to a significant reduction in complexity of the design but also accommodates stability analysis despite the presence of unknown quantities that tend to complicate it otherwise. Simulation results on 50 HP benchmark system show that

the proposed controller performs well under both transient and steady-state conditions using only estimates of unknown quantities. Furthermore, the simplification in the design and analysis is obtained without compromising the overall dynamic performance. Finally, it is worth highlighting that the simplification achieved by employing a reduced-order model can be utilized in analysing more complex issues in IM speed control such as parametric uncertainties, sensorless operation, time-delay issues, fault tolerant control, or effects of saturation, to name a few. These issues along with an experimental validation of the results pose as interesting future directions for this work.

Disclosure statement

No potential conflict of interest was reported by the authors.

Funding

The authors gratefully acknowledge the support and the constant help of the Deanship of Scientific Research at King Fahd University of Petroleum and Minerals. This work is under the KFUPM DSR grant referenced: IN131043. The financial support from King Abdulaziz City for Science and Technology (KACST) via KACST-TIC in Solid State Lighting [grant no. EE2381] and [KACST TIC R2-FP-008] is gratefully acknowledged.

ORCID

A. Sabir  <http://orcid.org/0000-0002-1010-9101>

References

- [1] Blaschke F. The principle of field orientation applied to the new transvector closed-loop control system for rotating field machines. *Siemens Rev.* 1972;34:217–220.
- [2] Akin B, Bhardwaj M. Sensored field oriented control of 3-phase induction motors. Texas instrument application report SPRABP8; 2013.
- [3] Krause PC, Wasynczuk O, Sudhoff SD, et al. Analysis of electric machinery and drive systems. Hoboken (NJ): Wiley; 2013.
- [4] Bodson M, Chiasson J, Novotnak R. High-performance induction motor control via input–output linearization. *IEEE Control Syst.* 1994;14(4):25–33.
- [5] Fekih A, Chowdhury FN. On nonlinear control of induction motors: comparison of two approaches. *American Control Conference.* Vol. 1; 2004. p. 1135–1140.
- [6] Kwan CM. Robust adaptive control of induction motors. *Int J Control.* 1997;67(4):539–552.
- [7] Rao S, Utkin V, Buss M. Design of first- and second-order sliding mode observers for induction motors using a stator-flux model. *Int J Control.* 2010;83(7):1457–1464.
- [8] Ahmed-Ali T, Lamnabhi-Lagarrigue F, Ortega R. A semiglobally stable adaptive field-oriented controller for current-fed induction motors. *Int J Control.* 1999;72(11):996–1005.
- [9] Barambones O, Alkorta P. Vector control for induction motor drives based on adaptive variable structure control algorithm. *Asian J Control.* 2010;12(5):640–649.
- [10] Trabelsi R, Khedher A, Mimouni MF, et al. Backstepping control for an induction motor using an adaptive sliding rotor-flux observer. *Electr Power Syst Res.* 2012;93:1–15.
- [11] Saab SS. A stochastic iterative learning control algorithm with application to an induction motor. *Int J Control.* 2004;77(2):144–163.
- [12] Tomei P, Verrelli C. Learning control for induction motor servo drives with uncertain rotor resistance. *Int J Control.* 2010;83(7):1515–1528.
- [13] Li J, Ren HP, Zhong YR. Robust speed control of induction motor drives using first-order auto-disturbance rejection controllers. *IEEE Trans Ind Appl.* 2015;51(1):712–720.
- [14] Yuhua W, Jianlin M. Based on fuzzy PID control of AC induction motor vector control system. In: Jin D, Lin S, editors. *Advances in electronic commerce, web application and communication.* Heidelberg: Springer; 2012. p. 227–232.
- [15] Hoo CL, Haris SM, Chung ECY, et al. New integral antiwindup scheme for PI motor speed control. *Asian J Control.* 2015;17(6):2115–2132.
- [16] Fekih A, Chowdhury FN. A nonlinear state feedback controller for induction motors. *Electr Power Compon Syst.* 2005;33(11):1211–1227.
- [17] Retiere N, Foggia A, Roye D, et al. Deep-bar induction motor model for large transient analysis under saturated conditions. 1997 IEEE International Electric Machines and Drives Conference Record; IEEE; 1997. p. MD1/3.1–MD1/3.3.
- [18] Marino R, Tomei P, Verrelli CM. Induction motor control design. London: Springer; 2010.
- [19] Glumineau A, de León Morales J. Sensorless AC electric motor control. Cham: Springer International Publishing; 2015. (*Advances in industrial control*).